

**Reviewer #2:**

## Comments and Suggestions for Authors:

1. This paper investigates the formation of a deep convective boundary layer on June 6, 2022, at the southern edge of the Taklimakan Desert and the northern foot of the Tibetan Plateau, using coherent Doppler wind lidar (CDWL) and ERA5 reanalysis data. The study reveals the critical role of low-level jets and thermal effects in the development of the boundary layer, providing significant scientific insights into the transport of dust aerosols and the thermodynamic processes of the atmospheric boundary layer. Overall, this paper is well-written, scientifically rigorous, and presents strong conclusions with high publication value. I recommend it for publication after some additional details and further analysis are addressed.

**Response:** Thank you for your recognition of this work. The manuscript has been greatly improved with your comments.

2. The paper does not provide a detailed explanation of how the boundary layer height is estimated using Equation (1) in the methods section. It is recommended that the authors provide a more detailed explanation of how the boundary layer height is derived.

**Response:** Thank you very much for this professional suggestion. We have made a more detailed for the calculation process of BLH in Sect. 2. and we have introduced the data processing method of CDWL in the Appendix B of the manuscript.

**Change:** P4L20-P5L9. “Based on this, the TKEDR threshold method can effectively estimate the BLH (Wang et al., 2021; Banakh et al., 2021).

The calculation formula of TKEDR is as follows (Banakh and Smalikho, 2018):

$$TKEDR = \left[ \frac{\overline{D}_L(\varphi_l) - \overline{D}_L(\varphi_1)}{A(l\Delta y_k) - A(\Delta y_k)} \right]^3 \quad (1)$$

where  $\overline{D}_L(\varphi_l)$  is azimuth structure function.  $L$  is the serial number for the laser beam's line of sight.  $\varphi_l = l\Delta\theta$ ,  $\Delta\theta$  is the azimuth angle resolution, and  $l=1,2,3,4,\dots$ . The  $A(l\Delta y_k)$  is calculated theoretically for the Kolmogorov model of the two-dimensional turbulence spectrum (Banakh et al., 2017), and  $\Delta y_k$  is the transverse dimension of the probed volume, and  $k$  is the range gate number,  $k=1,2,3,\dots$ . The error analysis for calculating TKEDR and MLH was conducted by Viktor A. Banakh (Banakh et al., 2017; Banakh et al., 2021).

In this experiment, the value of  $l$  is set to 2, and the threshold of TKEDR is set to  $10^{-4} \text{ m}^2 \text{ s}^{-3}$ . When the location is at the height of  $H_n = \Delta R * N$  ( $N$  is the index number of bins, and  $\Delta R$  is radial spatial resolution), if all TKEDR values within the range  $[\Delta R * (N+1), \Delta R * (N+5)]$  are less than the threshold, then  $H_n$  is used as the BLH”.

P5L26. “When the CNR value is below -17 dB, the calculated products are eliminated in the preprocessing”.

P18L6-P19L1. “The CNR is obtained by the ratio of the signal area to the noise area of the power spectrum (Fujii and Fukuchi, 2005):

$$CNR = A_s / A_n \quad (B1)$$

where  $A_s$  is the signal area of the power spectrum,  $A_n$  is the noise area of the power spectrum.

The line of sight velocity ( $V_{los}$ ) of CDWL is given by the following formula:

$$V_{los} = \lambda f_i / 2 \quad (B2)$$

where  $\lambda$  is the central wavelength of the emitted laser,  $f_i$  is the Doppler frequency shift for aerosols.

The wind vector in the atmosphere can be expressed by  $\vec{V}$ :

$$\vec{V} = (u, v, w) \quad (B3)$$

$u, v, w$  represent the north-south velocity, east-west velocity, and vertical velocity, respectively.

When using Velocity Azimuth Display (VAD) scanning mode, the direction vector  $\vec{S}$  can be expressed as:

$$\vec{S} = (\cos\theta\cos\varphi, \sin\theta\cos\varphi, \sin\varphi) \quad (B4)$$

Where  $\theta$  is the azimuth angle of the laser beam, and  $\varphi$  is the elevation of the laser beam.

From formula B2, B3, and B4, it can be concluded that (Browning and Wexler, 1968):

$$V_{los} = \vec{V} \cdot \vec{S}_m \quad (B5)$$

From formula B5,  $u, v, w$  can be calculated. The horizontal wind direction is calculated as follows:

$$WD = \arctan(u, v) \quad (B6)''.$$

3. The paper mentions the impact of the downhill airflow on the low-level jet and the inversion layer but lacks specific observational data and analysis. On page 5, line 21, the paper states: "At 0:00 LT~6:00 LT, before the formation of the LLJ, the downhill airflow blowing from the TP to the desert was superimposed on the desert background wind field." However, Figure 3e shows that the region is dominated by north and northeast winds, suggesting that the descending airflow is likely not from the Tibetan Plateau. Additionally, based on Figure 4, I believe that the local temperature drop is more likely due to the transport of cooler air from the upstream of the jet stream. It is recommended that the authors provide more information on the downhill airflow to make it easier for readers to understand.

**Response:** Thank you for your kind reminder. The geographical location of the study site is shown in the following figure, and the study site located at the northern foot of the Tibetan Plateau. The northeast part of the study site is blocked by the Tibet Plateau. In this manuscript, first of all,  $0^\circ$  represents the wind blows to the north. From 0:00 LT to 6:00 LT, the wind direction above 3 km is approximately distributed between  $225^\circ$  and  $295^\circ$  (Fig. 3e), and there is a clear sinking airflow in the horizontal wind speed figure (Fig. 3b). Secondly, it can be seen from the wind vectors in Fig. 4(a-c) that the upstream wind speed of the study site is very small, but after reaching the study site, it changes to a strong easterly wind, and the potential becomes lower (Fig. 4h), which can demonstrate the superposition effect of the downhill airflow. Finally, combined with the geographical location map, it can be seen that the superposition effect of the downhill airflow on the Tibetan Plateau induces the formation of LLJ.

It's worth noting that the cooling at the study site is also affected by cold air transported by the upstream of the LLJ, we have also added some discussion on this in the manuscript.

**Change:** P6L6-8, "It can be clearly found in Fig. 3b that the horizontal wind speed has subsided from 4 km to 2 km, and the wind is the downhill wind blowing from the TP to the desert (Fig .3e, >3 km,  $225^\circ$ - $295^\circ$ ). When the downhill airflow was superimposed on the desert background wind field".

P6L14-15, "with the cold downhill airflow and the upstream cold airflow traveled to the desert basin where the study site is located".

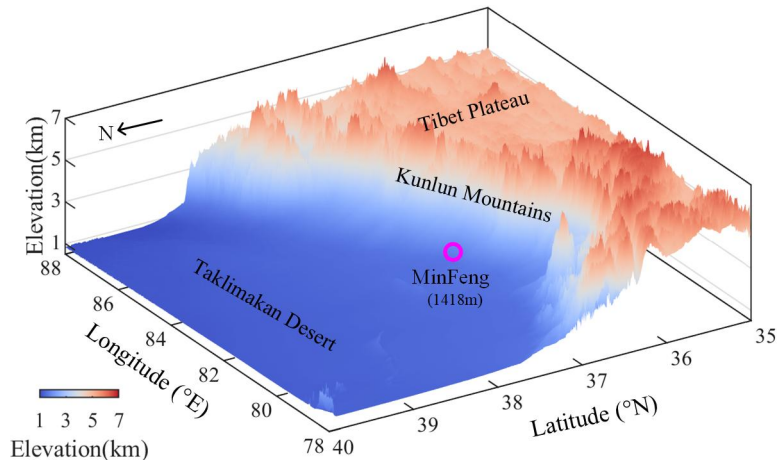


**Figure C1.** The 3D topographic map of the study area, and the purple circle represent the study site of MinFeng

4. The paper mentions that dust aerosols have an impact on surface and atmospheric temperatures but lacks specific quantitative analysis. Providing the diurnal variation of dust concentration could more intuitively show the impact of dust concentration changes on the boundary layer.

**Response:** Thank you very much for this professional suggestion. The MinFeng station was built in 2018. At present, there is still a lack of data reflecting dust concentration such as PM<sub>10</sub> on the day of the experiment. However, the CNR (Fig. 3a) can be used as indirect indicators of dust concentration, and they reflect the distribution of dust concentration. For example, “the atmosphere exhibited a stratified state (Blackadar, 1957), so that the high concentration of CNR values was distributed below 1 km, which can provide a material basis for boundary layer development”, “it can be seen that the values of TKEDR were consistently maintained at a high level, indicating a significant enhancement in the vertical transport capacity of the atmosphere (Wang et al., 2020). Consequently, the underlying CNR value below 1 km in Fig. 3a increased significantly”.

**Change:** P5L25-26. “The CNR can be used as an indicator of aerosol concentration (Pea et al., 2013)”. P6L27-28. “the atmosphere exhibited a stratified state (Blackadar, 1957), so that the high concentration of CNR values was distributed below 1 km, which can provide a material basis for boundary layer development”.

P7L1-3. “it can be seen that the values of TKEDR were consistently maintained at a high level, indicating a significant enhancement in the vertical transport capacity of the atmosphere (Wang et al., 2020). Consequently, the underlying CNR value below 1 km in Fig. 3a increased significantly”.

5. An interesting phenomenon can be observed in Figure 2, where higher boundary layers occur more frequently in spring and summer. Therefore, are the effects of the low-level jet and thermal effects on the deep convective boundary layer proposed in this study seasonal? We look forward to the authors addressing this question in the discussion section.

**Response:** It is my pleasure to discuss this with you. The following figure shows the wind frequency rose during a 2-year period at the study site. In spring, firstly, the temperature of the underlying surface rises rapidly after being heated by solar radiation, which accelerates the freeze-thaw alternation of the soil. Secondly, the east-west airflows converge here, making it the most frequent location for dust storm disaster in China, and the boundary layer also develops vigorously. Finally, according to the principle of inertial oscillation, the LLJ of east direction prevails in spring. In summer, the strong

westerly wind dominates the study site, and the characteristics of the dust underlying surface have the most significant heating effect on the atmosphere, resulting in strong convection and turbulent activity during the daytime, which is conducive to the formation of deep CBL. In terms of LLJ formation, the first is that there is easy to form an inversion layer due to the rapid cooling of the dust underlying surface, so that the lower layer of the boundary layer is in a stable stratification and is conducive to the excitation of the inertial oscillation mechanism. Secondly, there is a large temperature difference between daytime and nighttime, as well as the different cooling amplitude on the slope terrain, which makes it easier for downhill airflow to form, thereby promoting the development of LLJ.

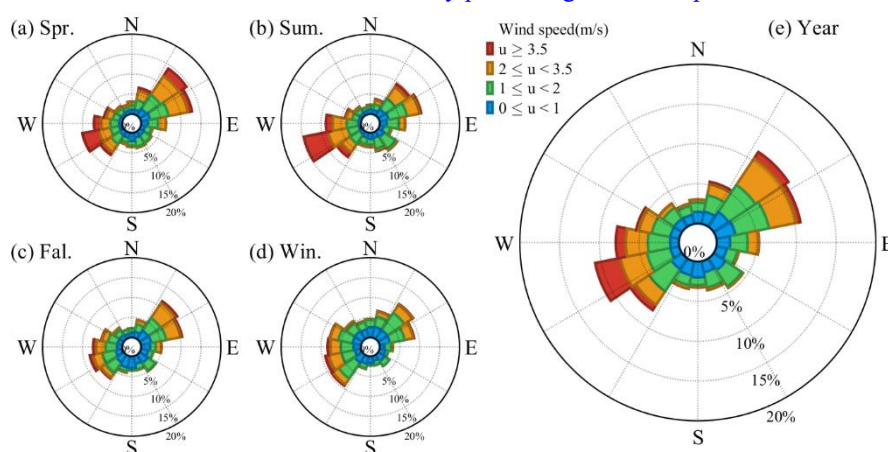


**Figure C2.** The rose diagram of wind frequency on the surface of study site from July 2021 to July 2023. The wind speed of 3.5 m/s can be used as the critical wind speed of blowing dust.

6. Why did the authors use sea level air pressure in the study? Sea level pressure is absent in TP and Taklimakan Desert due to the presence of terrain. Is it reasonable to use the difference in sea level pressure to analyze the formation of downhill airflow?

**Response:** Thank you for your question. Due to the high altitude and thin air of the Tibet Plateau, the local surface atmospheric pressure is generally lower than that of the desert basins. Sea level pressure refers to the atmospheric pressure per unit area calculated from the height of the sea level. Usually, in meteorological applications, atmospheric pressure values at different altitudes are typically converted to pressure values above sea level in order to establish standards and facilitate comparisons. Therefore, we have adopted sea level air pressure in this manuscript.

7. Other specific comments.

**Response:** Thank you for your kind reminding, we have carefully revised the manuscript. The clarity of the picture has also been improved. All changes made in the revised manuscript are marked in blue.

**Change:** P1L17-18. “During the stage of LLJ prior to the formation of the deep CBL, the LLJ had made sufficient preparations for the development of the deep CBL in terms of momentum, energy, and material.”

P1L20. “temperature inversion layer”.

P1L23. “During the stage of thermal effects, the sensible heat driven air-pump from the Tibet Plateau”.

P2L10-15. “These studies also revealed that the deep CBL exerts an influence on the local pollutant transmission and diffusion, cloud formation processes, strong convective weather, rainfall, drought and so on”.

P2L16-30. “For example, in the hinterland of the TD, the intense surface heating is not the primary

reason for the formation of deep CBL, whereas the presence of weak temperature inversion and near-neutral residual layer (RL) above the CBL are crucial (Zhang et al., 2022; Xu et al., 2018); The low-level jet (LLJ) can trigger significant air accumulation and dynamic convergence in the lower-level atmosphere, while the deep CBL is usually accompanied by the LLJ on the following night (Wang et al., 2019); The deep CBL enables the formation of clouds in the late afternoon, the formation of clouds will not only lead to a significant cooling of surface, but also make the momentum in the upper part of the boundary layer to transport downward and cause dust emissions (Zhang et al., 2024). Due to the fact that the TaZhong station is located in the center of the TD, and is equipped with the most comprehensive observation equipment, most studies of deep CBL are concentrated here. However, the MinFeng station, which is located on the northern slope of the Tibet Plateau (TP) and has severe wind-sand activities (Yang et al., 2016; Xiao et al., 2008), was established in 2018 (Yang et al., 2020). On the one hand, there is a lack of sufficient study results of deep CBL, and the particularity of geographical locations (TD, slope terrain, Kunlun Mountains, TP) further complicates the formation mechanism of deep CBL. On the other hand, the deep CBL plays an important role in the regional circulation and weather, its study not only helps to reveal the mechanism of local dust emission and transport (Jia et al., 2015; Meng et al., 2019), but also promotes the understanding of the land-atmosphere interaction between the TD and the TP.”.

...